Biochimica et Biophysica Acta 1848 (2015) 1514–1523

Contents lists available at ScienceDirect

Biochimica et Biophysica Acta

journal homepage: www.elsevier.com/locate/bbamem

The *E2*P-like state induced by magnesium fluoride complexes in the Na,K-ATPase. Kinetics of formation and interaction with Rb^+ ☆

Mónica R. Montes *, Mariela S. Ferreira-Gomes, Mercedes Centeno, Rolando C. Rossi

Instituto de Química y Fisicoquímica Biológicas and Departamento de Química Biológica, Facultad de Farmacia y Bioquímica, Universidad de Buenos Aires, Junín 956, 1113 Buenos Aires, Argentina

ARTICLE INFO

Article history:
Received 5 December 2014
Received in revised form 19 March 2015
Accepted 23 March 2015
Available online 30 March 2015

Keywords:
P-type ATPases
Crystallized Na
K-ATPase
*E2*P-like states
Magnesium fluoride complex
Rb^+ occlusion

ABSTRACT

The first X-ray crystal structures of the Na,K-ATPase were obtained in the presence of magnesium and fluoride as *E2*(K_2)Mg–MgF_4, an *E2*·Pi-like state capable to occlude K^+ (or Rb^+). This work presents a functional characterization of the crystallized form of the enzyme and proposes a model to explain the interaction between magnesium, fluoride and Rb^+ with the Na,K-ATPase. We studied the effect of magnesium and magnesium fluoride complexes on the *E1*–*E2* conformational transition and the kinetics of Rb^+ exchange between the medium and the *E2*(Rb_2)Mg–MgF_4 state. Our results show that both in the absence and in the presence of Rb^+, simultaneous addition of magnesium and fluoride stabilizes the Na,K-ATPase in an *E2* conformation, presumably the *E2*Mg–MgF_4 complex, that is unable to shift to *E1* upon addition of Na^+. The time course of conformational change suggests the action of fluoride and magnesium at different steps of the *E2*Mg–MgF_4 formation. Increasing concentrations of fluoride revert along a sigmoid curve the drop in the level of occluded Rb^+ caused by Mg^{2+}. Na^+-induced release of Rb^+ from *E2*(Rb_2)Mg–MgF_4 occurs at the same rate as from *E2*(Rb_2) but is insensitive to ADP. The rate of Rb^+ occlusion into the *E2*Mg–MgF_4 state is 5–8 times lower than that described for the *E2*Mg–vanadate complex. Since the *E2*Mg–MgF_4 and *E2*Mg–vanadate complexes represent different intermediates in the *E2*-P → *E2* dephosphorylation sequence, the variation in occlusion rate could provide a tool to discriminate between these intermediates.

© 2015 Elsevier B.V. All rights reserved.

1. Introduction

Na,K-ATPase is a representative member of the P-type ion-transporting ATPases. By using the energy derived from ATP hydrolysis into ADP and inorganic phosphate, Pi, this enzyme generates electrochemical gradients for Na^+ and K^+ across the plasma membranes of animal cells.

During the transport cycle the Na,K-ATPase can assume two principal conformations: *E1*, with high affinity for Na^+ and ATP, and *E2*, with high affinity for K^+ and low affinity for the nucleotide. Under physiological conditions (steps 1 through 6 in Fig. 1), *E1*ATP binds intracellular Na^+ and forms the phosphorylated *E1*P(Na_3) state, with release of ADP. After a conformational transition to *E2*P, Na^+ is released and extracellular K^+ binds and remains exchangeable with the medium until Pi dissociates, leaving K^+ occluded in *E2*. Occluded K^+ is then released into the cytoplasmic medium after the binding of ATP [1] (steps 4 through 6 in Fig. 1). Mg^{2+} is an essential ligand for the functioning of the transport cycle, particularly for the phosphorylation by ATP, and also for the backward phosphorylation by Pi (step 9 in Fig. 1).

Fluorinated complexes such as magnesium fluoride, aluminum fluoride and beryllium fluoride are widely used to inhibit the activity of many types of enzymes [2–5]. These small inorganic molecules have been extensively employed for structural analysis of the *E2*P states of the Ca-ATPase [2,3,6,7], since they seem to imitate the phosphoryl group in the ground (beryllium fluoride), transition (aluminum fluoride, which is similar to vanadate) and product (magnesium fluoride) states during the physiological pathway of dephosphorylation:

E2-P (ground state) → *E2*·P (transition state) → *E2*·Pi (product state) → *E2* + Pi.

The first X-ray crystal structures of the Na,K-ATPase were obtained in the presence of potassium (or rubidium), magnesium and fluoride as *E2*(K_2)Mg–MgF_4, an *E2*·Pi-like state capable to occlude K^+ (or Rb^+) [8,9]. The effects of several fluoride analogues on the Na,K-ATPase seem to be similar to those observed in the Ca-ATPase [3,10] but the interactions between these inhibitors and the sodium pump are less characterized. One of the first works was presented by Murphy and Hoover [3] who proposed that Na,K-ATPase with Mg^{2+} or Mg^{2+} and K^+ bound, forms an inactive complex with fluoride and more recently Cornelius et al. [11] analyzed the inhibition of the sodium pump by metal–fluoride

☆ This work was supported by grants from Consejo Nacional de Investigaciones Científicas y Técnicas (PIP 0706), Agencia Nacional de Promoción Científica y Tecnológica (PICT 2012-1053) and Universidad de Buenos Aires, Argentina (W 307). MC is an undergraduate student of the University of Buenos Aires, and MFG, MRM and RCR are established investigators from Consejo Nacional de Investigaciones Científicas y Técnicas.

* Corresponding author. Tel.: +54 11 4 964 5506; fax: +54 11 4 962 5457.
E-mail address: mmontes@qb.ffyb.uba.ar (M.R. Montes).

http://dx.doi.org/10.1016/j.bbamem.2015.03.023
0005-2736/© 2015 Elsevier B.V. All rights reserved.

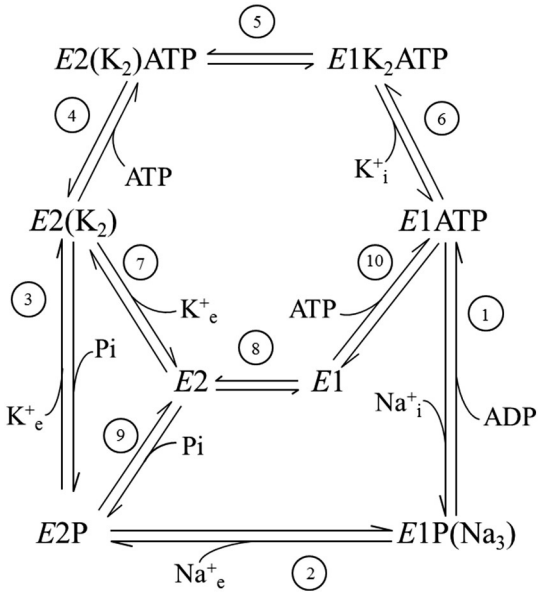

Fig. 1. A simplified version of the Albers–Post model for the functioning of Na,K-ATPase. The subscripts "**i**" and "**e**" mean intracellular or extracellular.

complexes. However, it is unclear the mechanism by which the *E*2(Rb$_2$)Mg–MgF$_4$ state is formed. Therefore, formation of the inactive complex probably requires a multistep reaction where Mg^{2+}, F^-, and/or known stable compounds of magnesium fluoride bind to the phosphorylation domain of the Na,K-ATPase.

The *E*2(Rb$_2$)Mg–MgF$_4$ structure contains two magnesium ions, one as the central ion of the MgF_4^{2-}, complex and a second one, as in the case of Pi, AlF_4^- and BeF_3^-, for establishing proper coordination interactions between these complexes and the phosphorylation site in *E*2 [8,9]. It is therefore unavoidable that formation of *E*2(Rb$_2$)Mg–MgF$_4$ occurs to some degree when studying the effects of fluoride complexes with aluminum and beryllium on the enzyme. Besides the role of Mg^{2+} to form the *E*2P-like complexes, it is a well-known fact that this cation binds to the Na,K-ATPase stabilizing the enzyme in the *E*1 conformation [12], opposing the effect exerted by the Mg^{2+}–fluoride complex.

This work presents a functional characterization of the crystallized *E*2(Rb$_2$)Mg–MgF$_4$ form of the enzyme and proposes a model to explain the interaction between magnesium, fluoride and Rb^+ with the Na,K-ATPase to form this *E*2·Pi-like state. With this aim, we evaluated the effects of Mg^{2+} and Mg^{2+}–fluoride complexes on the *E*1–*E*2 conformational changes using the fluorescence probe eosin. This probe binds to the nucleotide site of the Na,K-ATPase with high affinity when the dephosphorylated enzyme is in the *E*1 conformation, producing an increase in fluorescence signal [13,14]; the transition to *E*2 or *E*2P-like states (see steps 8 and 9 in Fig. 1) can thus be monitored as a fluorescence decay. Additionally, by measuring Rb^+ occlusion we evaluated the kinetics of Rb^+ exchange between the medium and the *E*2(Rb$_2$)Mg–MgF$_4$ state.

2. Materials and methods

2.1. Enzyme and reaction conditions

Na,K-ATPase was partially purified from pig kidney according to Klodos et al. [15] and kindly provided by the Department of Biophysics, University of Århus, Denmark. The specific activity at the time of preparation was 23–25 (μmol of Pi) min^{-1} (mg of protein)$^{-1}$ measured under optimal conditions (150 mM NaCl, 20 mM KCl, 3 mM ATP, and 4 mM $MgCl_2$ in 25 mM imidazole–HCl, pH 7.4 at 37 ° C). Incubations were performed at 25 °C in media containing 25 mM imidazole–HCl (pH 7.4 at 25 °C) and 0.25 mM EDTA. The concentrations of other components varied according to the experiments and are indicated in each figure legend.

2.2. Materials

[^{86}Rb]RbCl ($^{86}Rb^+$) was obtained from Perkin-Elmer NEN Life Sciences (USA). The fluorescent probe eosin (eosin-Y, free acid), ADP and NaF were from Sigma Chemical Co (USA). For some of the experiments, the fluoride solution was obtained as an imidazolium salt (ImF) by passing solutions of NaF through a column containing a cation exchange resin (Bio Rad AG MP-50) previously equilibrated with imidazole.

2.3. Magnesium fluoride compounds

MgF^+ is the only known ionic complex formed in aqueous solutions, with an equilibrium constant of formation of 63 M^{-1} at zero ionic strength [16]. Nevertheless, in a recent theoretical analysis Shibata et al. [17] have proposed the existence of the anionic complexes MgF_3^-, MgF_4^{2-} and MgF_5^{3-} in aqueous solution. If these complexes existed, an excess of F^- should prevent the precipitation of MgF_2 when the solubility product constant is surpassed. To test this, we performed experiments at 25 °C in the absence of enzyme in which $MgCl_2$ and NaF in different concentrations were mixed in media containing 25 mM imidazole–HCl (pH 7.4 at 25 °C) and 0.25 mM EDTA. The formation of a precipitate in the mixture was detected by turbidimetry at 340 nm in a spectrophotometer (Jasco V550) for 1 h of continuous recording. When media contained 5 mM $MgCl_2$, addition of NaF to final concentrations that ranged from 10 to 100 mM showed formation of turbidity; the higher the concentration of NaF the faster was the formation of the precipitate. In an independent experiment, we analyzed the total Mg concentration from the supernatant of media formed by mixing $MgCl_2$ (final concentration 5 mM) and different concentrations of NaF (see Supplementary data). Results show that total Mg concentration in the supernatant was 5 mM in the absence of fluoride and remained almost constant up to 10 mM NaF, and then decreased sharply at 25 mM NaF to levels that fall below the detection limits of the titration method for 100 and 150 mM NaF, showing no signs of re-dissolution of the crystals. These results suggest that MgF_4^{2-} is not formed under the conditions of our experiments.

2.4. Magnesium concentration

Concentration of free Mg^{2+} was measured using the dye arsenazo III, which forms complexes with certain divalent cations producing an altered absorption spectrum [18]. Absorbance at 618 and 514 nm was measured for solutions with 20 μM arsenazo and different concentrations of $MgCl_2$ and ImF. Results are shown in Fig. 2. Nonlinear regression analysis of data showed that a two step reaction,

$$Mg^{2+} + F^- \leftrightarrow MgF^+$$
$$MgF^+ + F^- \leftrightarrow MgF_2$$

with dissociation constants (mM) $K_1 = 9.74 \pm 0.34$ (S.E.) and $K_2 = 13.5 \pm 1.4$ (S.E.), respectively, was the best fitting model.

Total magnesium concentration ([total Mg^{2+}]) was calculated by subtracting [EDTA] from [$MgCl_2$].

2.5. E1–E2 conformational changes

The conformational states were studied by measuring the eosin fluorescence signal. Eosin binds to states in the *E*1 conformation, like *E*1 and *E*1Mg, with a K_d of 0.25–0.5 μM, producing an increase in fluorescence signal. The conversion to states in the *E*2 conformation, like *E*2(Rb$_2$) and the *E*2Mg–MgF$_4$ complex, can therefore be measured as a decrease in fluorescence. In equilibrium conditions, the membrane-bound Na,K-ATPase was

incubated with eosin in the presence of $MgCl_2$ and ImF. Eosin fluorescence was measured in a Jasco FP 6500 spectrofluorimeter with a band-pass of 3 nm. The excitation wavelength was 520 nm, and emission was measured at 540 nm. The time courses of conformational transitions were recorded in a Stopped–Flow Reaction Analyzer (SX-18MV, Applied Photophysics). In each experiment, 2000 data points were collected. Between 5 and 7 experimental traces were averaged to evaluate each time course. Control experiments showed no effect of fluoride, magnesium and magnesium fluoride on eosin fluorescence in the absence of protein. The enzyme was kept in the dark throughout the experiments with eosin.

2.6. Occluded Rb^+

This was measured according to Rossi et al. [19]. Briefly, reactions were carried out in a rapid-mixing apparatus (SFM4 from Bio-Logic, France) connected to a quenching and washing chamber that contained a Millipore filter. The filter was then removed, dried, and counted for radioactivity. Blanks were estimated from the amount of $^{86}Rb^+$ retained by the filters when the enzyme was omitted. Equilibrium occlusion of Rb^+ was attained by incubating enzyme during 40–60 min with $MgCl_2$, ImF and $^{86}Rb^+$. The time course of Rb^+ occlusion was measured after mixing one volume of enzyme suspension with one volume of a solution containing $^{86}Rb^+$ and incubated for different lengths of time. To measure the time course of Rb^+ deocclusion, one volume of enzyme suspension equilibrated with 500 μM $^{86}Rb^+$ was mixed with 19 volumes of a solution containing Na^+ and 500 μM of unlabeled Rb^+ as to cause a 20-fold decrease in the specific activity of $^{86}Rb^+$.

2.7. Data analysis

The equations were fitted to the experimental data by a nonlinear regression procedure based on the Gauss–Newton algorithm using commercial software (Excel 7.0 for Windows and Sigma-Plot 10.0 for Windows). To define the goodness of fit of a given equation to the experimental results we used the Second-Order Akaike Information Criterion (AIC_C) [20] and the best equation was chosen as that giving the lower value of AIC_C. Parameter values are expressed as mean ± standard error (S.E.). To obtain the simulated curves from the kinetic model, we used the program Copasi version 4.10 (University of Virginia) [21].

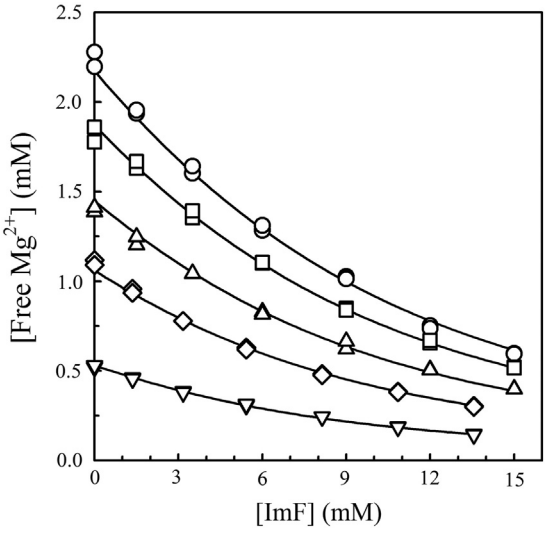

Fig. 2. Free magnesium concentration as a function of [ImF]. [Free Mg^{2+}] was determined for solutions with 2.2 (○), 1.8 (□), 1.4 (Δ), 1.1 (◊) and 0.5 (▽) mM [total Mg^{2+}]. Continuous lines represent the best fitting for the two step reaction model (see Materials and methods) with dissociation constants $K_1 = 9.74$ mM and $K_2 = 13.5$ mM, respectively.

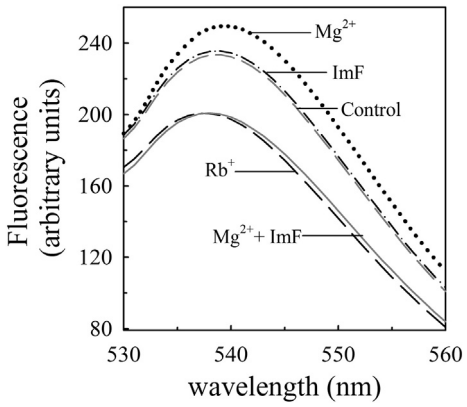

Fig. 3. Emission spectra of eosin fluorescence. The enzyme (45 μg enzyme protein/ml) was incubated in media containing 25 mM imidazole–HCl (pH = 7.4 at 25 °C), 0.25 mM EDTA and 0.4 μM eosin in the absence (Control) or in the presence of 2 mM $MgCl_2$ (Mg^{2+}), 5 mM ImF (ImF), 5 mM ImF plus 2 mM $MgCl_2$ (Mg^{2+} + ImF), or 500 μM RbCl (Rb^+).

3. Results

3.1. E1–E2 conformational changes

The conformational states of the Na,K-ATPase were studied by measuring the eosin fluorescence signal which is high for states in *E*1 and is low for states in *E*2 [13,14]. We examined the effect of the magnesium fluoride compounds on the states of the Na,K-ATPase under equilibrium conditions in the absence of other added cations. The enzyme was incubated in the presence of fluoride and magnesium. In one experiment Rb^+ was added as a control for the *E*2 conformation. It can be seen in Fig. 3 that, although addition of fluoride alone (ImF) doesn't change and magnesium alone (Mg^{2+}) increases the fluorescence signal (shifting the enzyme to the *E*1 conformation), the simultaneous addition of fluoride and magnesium decreases fluorescence to a value similar to that obtained with Rb^+, which would reflect the formation of the *E*2·Pi-like complex. This latter state, presumably *E*2Mg–MgF_4, corresponds to the first structure crystallized [8,9] but lacking K^+ and Rb^+. The stability of this *E*2·Pi-like complex is sufficient to prevent the enzyme to return to the *E*1 state upon Na^+ addition. Results in Fig. 4 show that during the time of the experiments, 6 mM Na^+ fails to produce a measurable shift to the *E*1 state when the enzyme was forming

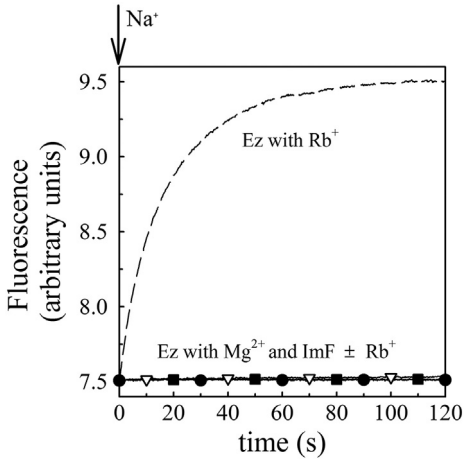

Fig. 4. Lack of effect of Na^+ in the presence of magnesium and fluoride. A suspension of Na,K-ATPase with eosin (final concentrations: 45 μg enzyme protein/ml, 0.32 μM eosin) was mixed with a medium containing NaCl. Experiments were performed starting with the enzyme in a medium with (final concentrations) 2 mM $MgCl_2$ and 5 mM ImF, either without (■) or with (●,▽) 100 μM RbCl, and mixing this suspension with 6 (●,■) or 60 (▽) mM Na^+. A control experiment (dashed line) was performed by adding Na^+ (6 mM, final concentration) to enzyme incubated with RbCl (100 μM, final concentration).

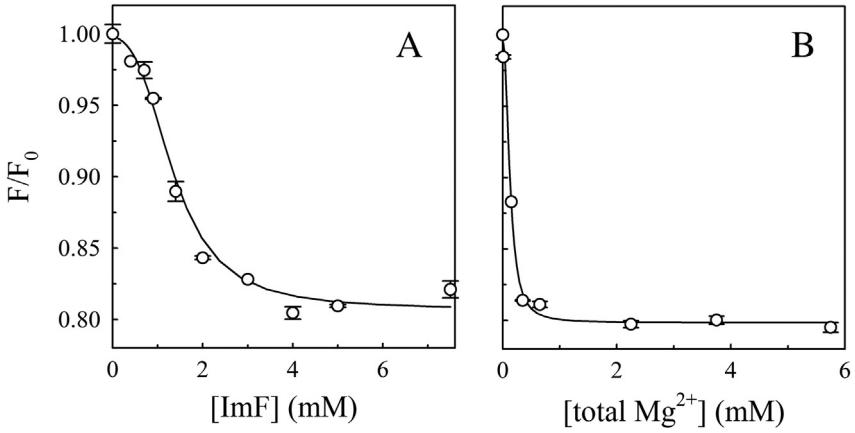

Fig. 5. Effects of Mg^{2+} and fluoride on the equilibrium between the *E*1 and the *E*2P-like states. Eosin fluorescence of Na,K-ATPase (45 μg enzyme protein/ml) incubated with 0.4 μM eosin in the presence of 2 mM $MgCl_2$ and different concentrations of ImF (Panel A) or in the presence of 5 mM ImF and different concentrations of total Mg^{2+} (Panel B). Continuous line in panel B represents a Hill equation of [total Mg^{2+}]. Data are expressed as the mean ± S.D. of 3 independent experiments.

a complex with magnesium and fluoride, both in the presence and in the absence of Rb^+. A similar result was observed using 60 mM Na^+.

When the Na,K-ATPase was incubated with 2 mM $MgCl_2$, increasing concentrations of fluoride reduced the equilibrium level of eosin fluorescence with a $K_{0.5}$ of 1.35 ± 0.057 mM (Fig. 5A). This effect can be described by a sigmoid curve that might be reflecting the need of more than one fluoride ion [8] to form the complex with the enzyme. On the other hand, in media with 5 mM fluoride, increasing concentrations of Mg^{2+} (Fig. 5B) also decreased fluorescence and data could be fitted by a Hill equation with $K_{0.5} = 0.131 \pm 0.006$ mM and $n_H = 2.2 \pm 0.3$.

To evaluate the kinetics of the change from the *E*1 conformation to the *E*2Mg–MgF_4 state, a volume of enzyme with Mg^{2+} was mixed with a volume of a solution containing fluoride. Experiments were performed for ImF concentrations from 0.25 to 6.5 mM and $MgCl_2$ from 0.3 mM to 6 mM. Time courses in Figs. 6A–B and 7A–B show that, despite that more than 500 s are required to achieve equilibrium, a rapid component can also be observed within the first 5 s. A control experiment was performed to test whether the fast component could be due to a sudden drop in free Mg^{2+} concentration as a result of the dilution and/or combination with F^- of the magnesium present in the medium containing enzyme (Fig. 6C). However, when magnesium was included in both syringes in order to keep constant the concentration of free Mg^{2+} (data in Fig. 2 were used for this purpose) the time course still displayed a fast phase.

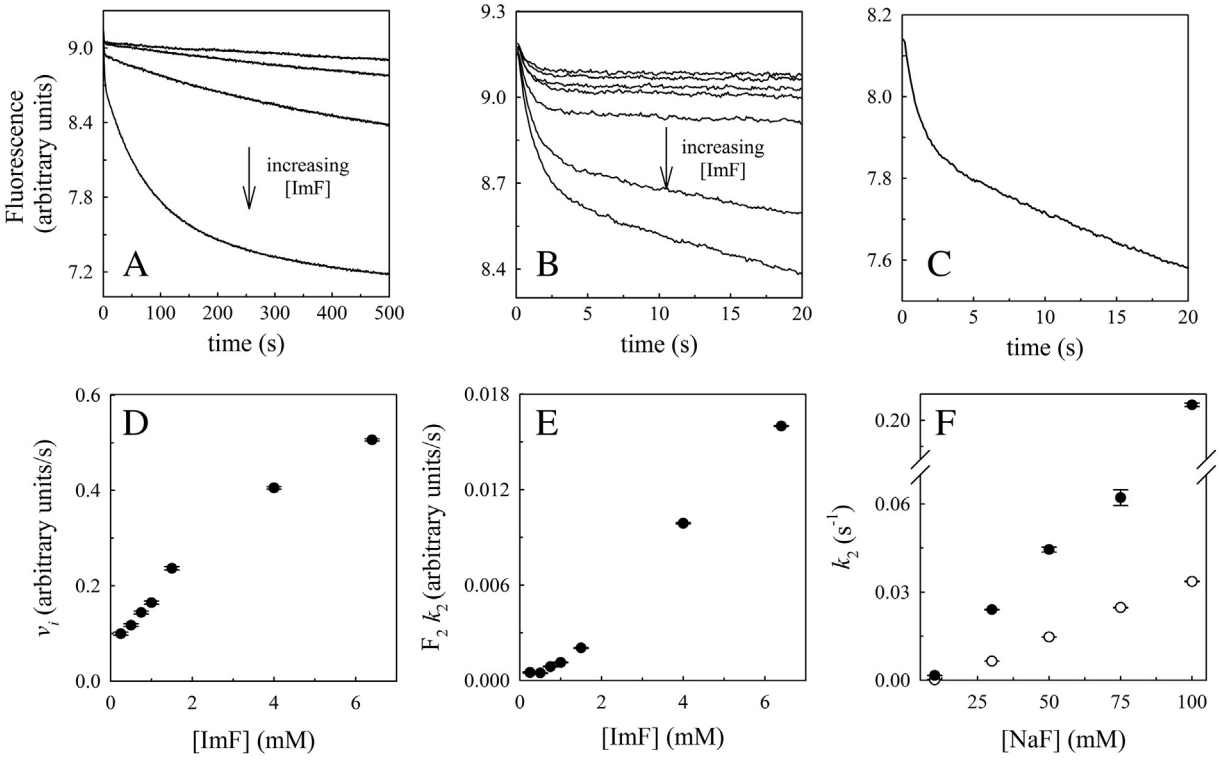

Fig. 6. Kinetics of the *E*1 → *E*2P-like state transition at different fluoride concentrations. One volume of the enzyme suspension with $MgCl_2$ was mixed (time = 0) with one volume of a medium containing different concentrations of ImF. Time courses of fluorescence change are shown in Panel A, spanning up to 500 s, and in Panel B, exploring the first 20 s. Final media contained 45 μg enzyme protein/ml, 2 mM $MgCl_2$, 0.32 μM eosin and 0.25, 0.75, 1.5 and 6.4 mM ImF (Panel A) or 0.25, 0.5, 0.75, 1, 1.5, 4 and 6.4 mM ImF (Panel B). Panel C shows a time course for a similar experiment but where the concentration of free Mg^{2+} was kept constant (1.05 mM) by the addition of magnesium in the syringe containing ImF. v_i and $F_2 \times k_2$ (values ± 1 SE) calculated from the fitted values in Eq. (1) are respectively shown in Panels D and E. Panel F shows k_2 as a function of [NaF] at 2 mM (○) and 5 mM (●) $MgCl_2$ in experiments where [Na^+] was kept constant by supplementing NaF with NaCl.

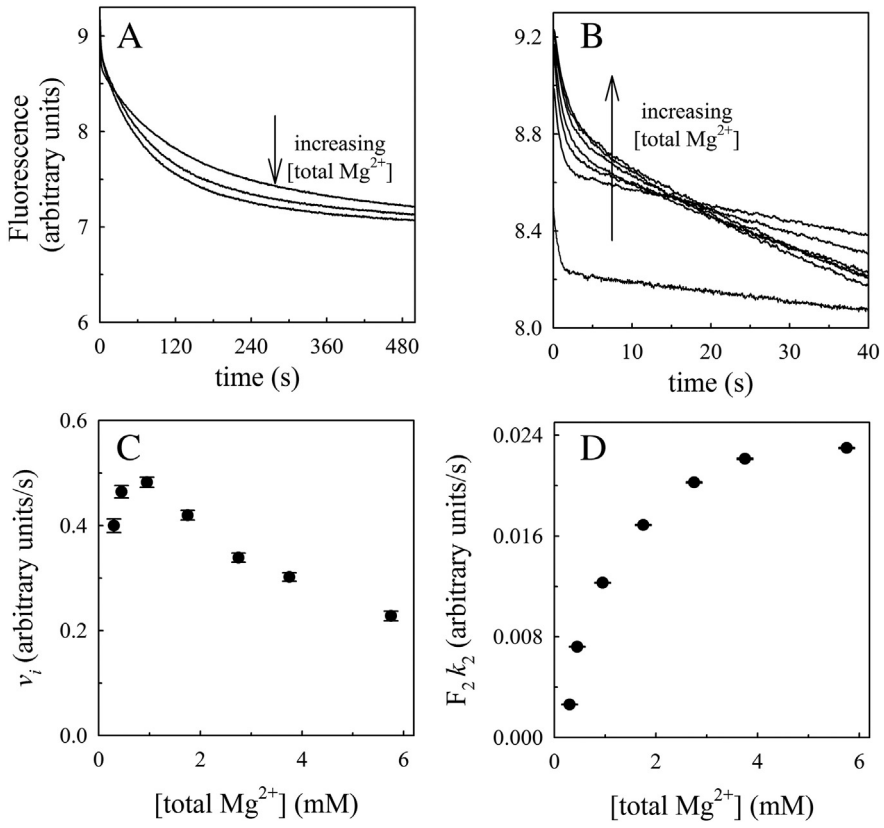

Fig. 7. Kinetics of the $E1 \rightarrow E2$P-like state transition at different magnesium concentrations. One volume of the enzyme suspension in different concentrations of $MgCl_2$ was mixed (time = 0) with one volume of a medium containing ImF. Time courses of fluorescence change are shown in Panel A, spanning up to 500 s, and in Panel B, exploring the first 40 s. Final media contained 45 μg enzyme protein/ml, 0.32 μM eosin, 5 mM ImF, and 0.95, 2.75 and 5.75 mM total Mg^{2+} (Panel A), and 0.3, 0.45, 0.95, 1.75, 2.75, 3.75 and 5.75 mM total Mg^{2+} (Panel B). v_i and $F_2 \times k_2$ (values ± 1 SE) calculated from the fitted values in Eq. (1) are respectively shown in Panels C and D.

The fluorescence time courses were adequately described by the sum of two exponential functions of time:

$$F = F_1 e^{-k_1 t} + F_2 e^{-k_2 t} + F_\infty \quad (1)$$

where the subscripts 1 and 2 represent the fast and slow components, respectively. From Eq. (1) it is possible to calculate the initial velocity of fluorescence change as $v_i = k_1 \times F_1 + k_2 \times F_2$, and that of the slow phase as $F_2 \times k_2$.

It can be seen that v_i increases with [ImF] along a curve that seems slightly concave downwards (Fig. 6D), possibly as the initial part of a hyperbolic curve, whereas $F_2 \times k_2$ increases with [ImF] along a parabolic curve (Fig. 6E) that would reflect the need of more than one fluoride ion to produce the effect. On the other hand, for increasing Mg^{2+} concentrations v_i raises and then decreases (Fig. 7C), whereas $F_2 \times k_2$ increases along a hyperbolic function (Fig. 7D). The dissimilar behaviors of v_i and $F_2 \times k_2$ suggest the existence of at least two different effects of fluoride and magnesium during the transition from the $E1$ forms to the $E2$·Pi-like state: while the fast component would be related to an early conformational redistribution from $E1$ to $E2$ states, the slow component is associated with the formation of the $E2Mg–MgF_4$ complex.

Cornelius et al. [11] reported that k_{obs} for the formation of an inhibited complex of the Na,K-ATPase with Mg^{2+} and fluoride (i.e. k_2 in our experiments) increased along a sigmoid saturating function of [NaF]. Given its implications on the mechanism of the process, we searched for signs of saturation by exploring fluoride concentrations higher than 6.5 mM. Fluorescence decrease was measured for [NaF] from 10 to 100 mM in experiments where the concentration of Na^+ was kept constant at 100 mM by supplementing NaF with NaCl. Under these conditions the fast phase was not observed and results could be fitted by a single exponential function of time. Results in Fig. 6F show that for the higher [NaF] tested, k_2 increases linearly and no tendency to saturation could be observed neither at 2 nor at 5 mM $MgCl_2$. Moreover, the slope of k_2 vs [NaF] in media with 5 mM $MgCl_2$ was 2.5 fold higher than in media with 2 mM $MgCl_2$.

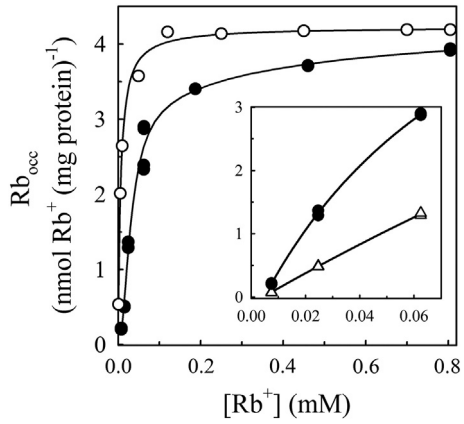

Fig. 8. Equilibrium levels of occluded Rb^+. Na,K-ATPase (45 μg enzyme protein/ml) was incubated with different concentrations of $^{86}Rb^+$ in the absence (○) or in the presence of 2 mM $MgCl_2$ plus 5 mM ImF (●). The inset shows Rb_{occ} in the presence of 2 mM $MgCl_2$ alone (△) or 2 mM $MgCl_2$ plus 5 mM ImF (●). Continuous lines represent a hyperbolic function of [Rb^+] in the absence of added ligands and a second-order rational function of [Rb^+] in the presence of Mg^{2+} and Mg^{2+} plus fluoride. Each experiment is representative of at least two independent experiments.

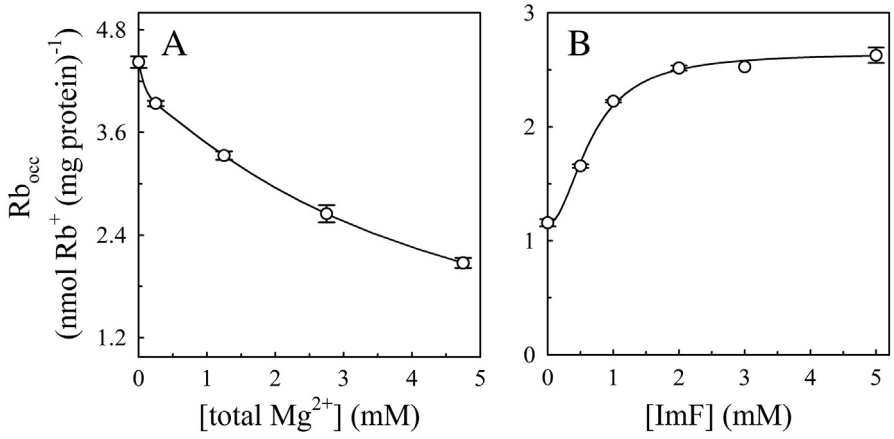

Fig. 9. Effect of fluoride and Mg^{2+} on the equilibrium levels of occluded Rb^+. Na,K-ATPase (45 μg enzyme protein/ml) was incubated with 65 μM $^{86}Rb^+$, ImF and $MgCl_2$. Panel A shows Rb_{occ} in the presence of 5 mM ImF as a function of [total Mg^{2+}]. Panel B shows Rb_{occ} in the presence of 2 mM $MgCl_2$ as a function of [ImF]. Data are expressed as the mean ± S.E. of 2 independent replicates in each experiment.

3.2. Rb^+ occlusion

The level of the state of the Na,K-ATPase holding occluded Rb^+ (Rb_{occ}) was measured in equilibrium conditions as a function of [Rb^+] in the absence (control) or in the presence of 2 mM $MgCl_2$ and 5 mM fluoride. From data in Fig. 8 it can be seen that in the medium containing magnesium and fluoride the $K_{0.5}$ was about 10-fold higher than that calculated for the control experiment (50 μM vs 5 μM) although the maximum occlusion capacity was not affected. On the other hand, at sub-saturating [Rb^+] the simultaneous addition of magnesium and fluoride reverted the decrease in Rb_{occ} produced by the addition of magnesium alone (inset in Fig. 8). These results are in line with those in Fig. 9, which shows that at constant [ImF], the increase in total Mg^{2+} concentration produced a decrease in Rb_{occ} (panel A), and that at constant [$MgCl_2$], addition of fluoride increased Rb_{occ} reaching a plateau at 3–5 mM ImF (panel B), probably because of the formation of the $E2(Rb_2)Mg–MgF_4$ complex and also in part because of the drop in free Mg^{2+}. It should be noted that the effect of Mg^{2+} observed in panel A is not accompanied by a conformational change to $E1$ (cf. Fig. 5B).

3.3. Rb^+ exchange through the extracellular (E2) or intracellular (E1) access

To investigate if magnesium fluoride stabilizes the Rb^+ occluded state, just as it does with the $E2$ conformation (see Fig. 4), we measured the effect of Na^+ on Rb^+ deocclusion. Fig. 10 shows that the time courses of Rb^+ release from $E2(Rb_2)$ or from $E2(Rb_2)Mg–MgF_4$ are similar. Both curves could be described by the sum of two exponential functions of time and the calculated initial velocity of Rb^+ deocclusion was (nmol Rb^+ s^{-1}) 0.21 ± 0.17 and 0.22 ± 0.13 in the absence and in the presence of magnesium fluoride, respectively. It has been proposed [22,23] that Rb^+ deocclusion in the absence of ATP occurs mainly through the extracellular access of the enzyme (when this is in the $E2$ conformation, step 7 in Fig. 1). To check Rb^+ release via the intracellular access we added ADP (here acting as an ATP analog, steps 4 through 6 in Fig. 1) in the deocclusion medium and measured the time course of Rb^+ release. Fig. 11 shows that magnesium fluoride completely prevents the acceleration of Rb^+ deocclusion caused by ADP, being the initial velocity in the presence of magnesium fluoride at least 20 fold lower than in its absence.

The time course of Rb^+ occlusion in the presence or in the absence of magnesium and fluoride is illustrated in Fig. 12. It can be seen that magnesium fluoride extremely decreased the initial rate of occlusion, which was 30 times lower than with magnesium alone and 3500 times lower than in the absence of both magnesium and fluoride.

4. Discussion

In this work we have studied the formation of the $E2$·Pi-like state from the Na,K-ATPase and magnesium fluoride compounds and the ability of this state to occlude the K^+-congener Rb^+. The use of the fluorescent probe eosin and stopped-flow fluorometry allowed easy and very precise measurements of the kinetics of the $E1 \rightarrow E2$ conformational change associated to the formation of this state. The main conclusions are: (i) the Na,K-ATPase is able to combine with magnesium and fluoride to form a very stable complex, presumably the $E2Mg–MgF_4$ state, that is in the $E2$ conformation even in the absence of Rb^+; (ii) the stability of this complex is such that its conversion to the $E1$ conformation upon addition of Na^+ cannot be detected in the time scale of minutes; (iii) the $E1 \rightarrow E2$ conformational change induced by F^- plus Mg^{2+} presents a time course with a rapid and a slow phase, of which only the latter seems to be related to the formation of the $E2Mg–MgF_4$ complex; (iv) it was not possible to detect saturation of the rate of formation of this complex by fluoride and magnesium, calling into question the proposal of the existence of a slow isomerization step subsequent to the binding of these ligands to the Na,K-ATPase; (v) the addition of fluoride reverts the action of Mg^{2+} on decreasing the equilibrium level of occluded Rb^+ by increasing the affinity for Rb^+; (vi) occlusion of Rb^+ into the $E2$·Pi-like complex is extremely slow; and (vii) the exchange of Rb^+ with $E2(Rb_2)Mg–MgF_4$ occurs

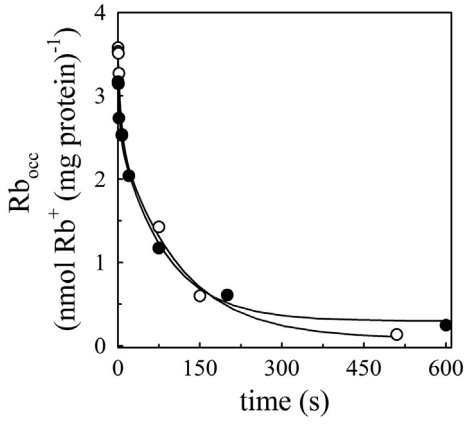

Fig. 10. The time course of Rb^+ release after Na^+ addition. Occluded $^{86}Rb^+$ remaining after a 20-fold dilution of the specific activity of $^{86}Rb^+$ was plotted as a function of time. Occluded Rb^+ was formed by incubating the enzyme with 500 μM $^{86}Rb^+$ in the absence (○) or in the presence of 5 mM ImF plus 2 mM $MgCl_2$ (●). Final media contained 27 μg enzyme protein/ml, 500 μM Rb^+ and 6 mM NaCl (○) and when present, 5 mM ImF and 2 mM $MgCl_2$ (●). Continuous lines represent the sum of two decreasing exponential functions of time. The data is representative of three independent experiments.

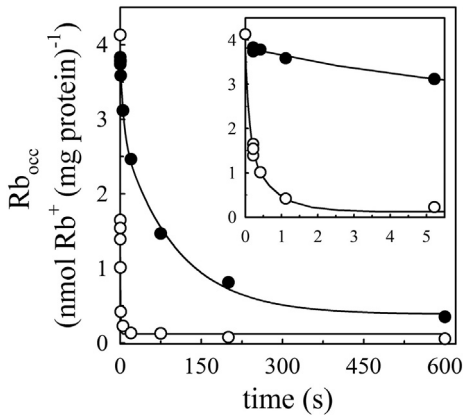

Fig. 11. Lack of effect of ADP on Rb^+ release in the presence of magnesium plus fluoride. Occluded $^{86}Rb^+$ remaining after a 20-fold dilution of the specific activity of $^{86}Rb^+$ was plotted as a function of time. Occluded Rb^+ was formed by incubating the enzyme with 500 μM $^{86}Rb^+$ in the absence (○) or in the presence (●) of 5 mM ImF plus 2 mM $MgCl_2$ Final media contained 27 μg enzyme protein/ml, 500 μM Rb^+, 6 mM NaCl and 3 mM ADP (○) and when present, 5 mM ImF and 2 mM $MgCl_2$ (●). The inset shows the first 5.5 s of the time courses. Continuous lines represent the sum of two decreasing exponential functions. The data is representative of three independent experiments.

mainly from *E*2, i.e. through the extracellular access, since the complex is incapable to shift to the *E*1 conformation.

4.1. Kinetics of conformational changes

Under equilibrium conditions, the changes in eosin fluorescence as a function of both fluoride and magnesium concentrations are comparable with the results obtained by Cornelius et al. [11] measuring inhibition of the ATPase activity. In agreement with the need of four fluoride and two magnesium ions to form the *E*2Mg–MgF_4 complex, the responses exhibit sigmoid shapes as a function of the concentration of both ligands. These authors reported values of $K_{0.5}$ of 0.133 mM (at 5 mM NaF) and 1.6 mM (at 5 mM $MgCl_2$) for magnesium and fluoride, respectively.

As pointed out under Results, there are indications that the two components observed in the time courses of fluorescence change are related to different phenomena: while the slow component would reflect the formation of *E*2Mg–MgF_4, the fast one seems to involve a re-equilibration between the states in the *E*1 and *E*2 conformations caused by fluoride addition.

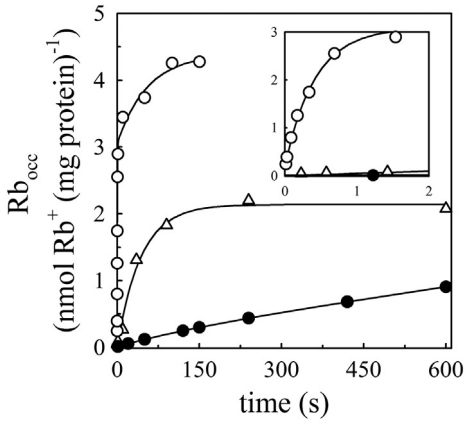

Fig. 12. Time courses of Rb^+ occlusion. The enzyme with no added ligands (○) or incubated with $MgCl_2$ (Δ) or with $MgCl_2$ plus ImF (●), was mixed with a solution containing $^{86}Rb^+$ for different lengths of time. Final media contained 45 μg enzyme protein/ml, 100 μM $^{86}Rb^+$ and when present, 2 mM $MgCl_2$ and 5 mM ImF. The inset shows the first 2 s of the time courses. Continuous lines represent the sum of two increasing exponential functions of time. The data is representative of at least two independent experiments.

The rate of the formation of *E*2Mg–MgF_4 increased along a parabolic function at low fluoride concentration (see also ref. [3]) and showed no signs of saturation within the range used in our experiments. However, Cornelius et al. [11] using concentrations of NaF up to 100 mM observed that k_{obs} increased along a sigmoid curve. In their experiments, Na^+ concentration varied together with that of F^- whereas in the experiments performed in this work, the concentration of Na^+ was kept constant at 100 mM. This raises the possibility that the saturation observed by Cornelius et al. was due to the fact that as Na^+ concentration increases, the enzyme is shifted to the *E*1 conformation thus decreasing the proportion of *E*2 and therefore the value of k_{obs}.

Regarding the analysis of the fast component of fluorescence change we propose that a complex between magnesium and fluoride (probably MgF^+) might combine to *E*1 producing an early redistribution of states in the *E*1 and *E*2 conformations. For this, *E*1MgF → *E*2MgF should be faster than *E*1 → *E*2 (see Fig. 13). A sudden drop in free Mg^{2+} concentration along with the assumption that the rate of *E*1 → *E*2 is faster than that of *E*1Mg → *E*2Mg is not a sufficient explanation for the phenomenon, since a significant fraction of the fast component remained present when the concentration of this cation was kept constant. The hypothesis of an early redistribution between states in *E*1 and *E*2 conformation agrees with the lack of a fast phase observed when the enzyme was incubated in media with 100 mM Na^+, where the equilibrium is strongly poised to *E*1. Free F^- can in principle be ruled out as the cause of the fast component since this anion is unable to modify by itself the *E*1–*E*2 equilibrium.

4.2. Magnesium fluoride compounds

Unlike aluminum and beryllium, which are described to form anionic complexes with fluoride in aqueous solution, there are no experimental evidence of anionic complexes formed by magnesium and fluoride [24] except for those belonging to compounds with macromolecules like G proteins [25] and P-type ATPases [2–4,6–11], among others. Our control experiments (see Materials and methods) confirmed that addition of an excess of F^- fails to produce re-dissolution of the precipitate formed by mixing magnesium and fluoride making very improbable the existence of a complex with one molecule of Mg^{2+} and four of F^- in aqueous solution. This leaves MgF^+ and MgF_2 (apart from Mg^{2+} and F^-) as the species of magnesium and fluoride available to combine with the enzyme. That brings to the hypothesis that the Na,K-ATPase and other P-type ATPases might be providing the required interactions in a high affinity site for the formation of *E*2Mg–MgF_4 from pieces of a complex ion,

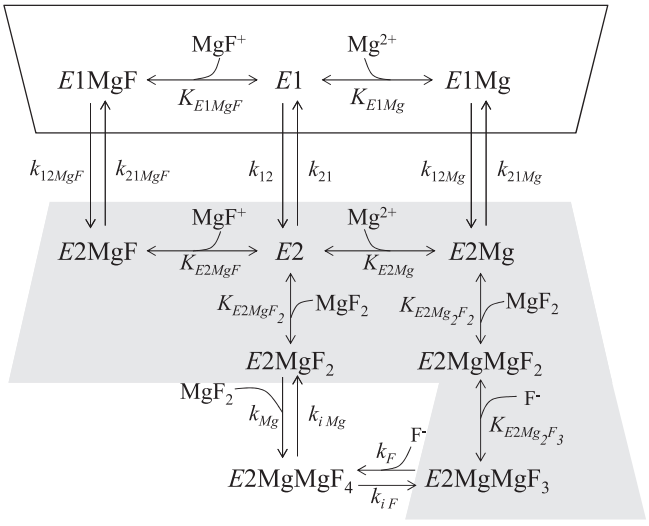

Fig. 13. A minimal model for the interaction between Na,K-ATPase, magnesium and fluoride. The enzyme exists in two main conformations, *E*1 and *E*2. Reactions that occur under rapid equilibrium conditions are indicated as.

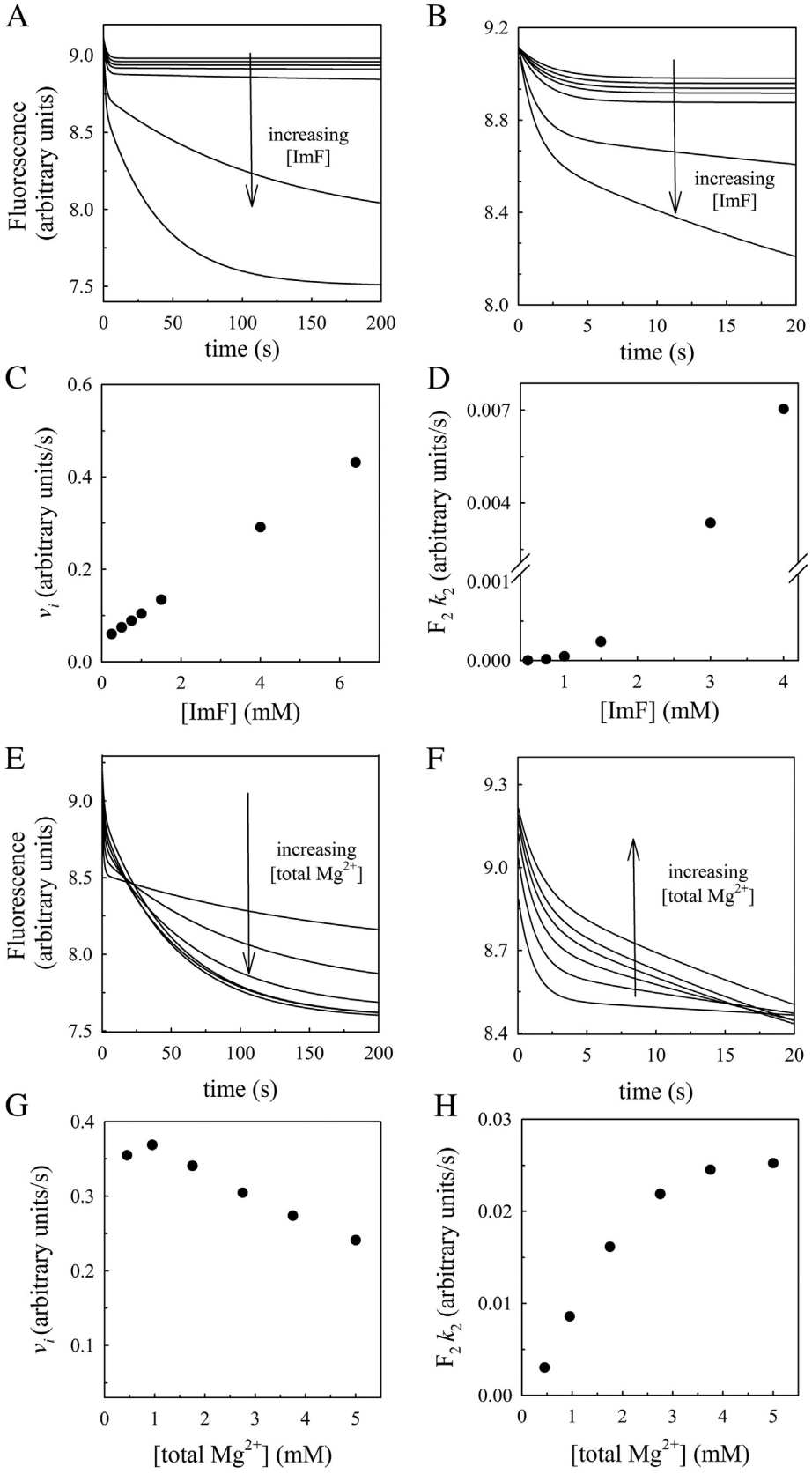

Fig. 14. Kinetics of conformational changes simulated according to the model shown in Fig. 13. The time courses at different [ImF] (Panels A and B) or different [total Mg^{2+}] (Panels E and F) were simulated using the following parameters' values: $K_{E1MgF} = 1$ mM, $K_{E1Mg} = 0.3$ mM, $k_{12MgF} = 1.95\ s^{-1}$, $k_{21MgF} = 0.62\ s^{-1}$, $k_{12} = 0.65\ s^{-1}$, $k_{21} = 0.49\ s^{-1}$, $k_{12Mg} = 0.01\ s^{-1}$, $k_{21Mg} = 0.052\ s^{-1}$, $K_{E2MgF} = 0.424$ mM, $K_{E2Mg} = 2.07$ mM, $K_{E2MgF2} = 100$ M, $K_{E2Mg2F2} = 1$ M, $K_{E2Mg2F3} = 24.9$ mM, $k_{iMg} = 0.0001\ s^{-1}$, $k_{Mg} = 9.94\ s^{-1}\ \mu M^{-1}$, $k_F = 1.28\ s^{-1}\ \mu M^{-1}$, $k_{iF} = 0.003\ s^{-1}$, $K_{MgF} = 9.23$ mM, $K_{MgF2} = 13$ mM. Eq. (1) was fitted to the simulated time courses. Calculated values of v_i and F_2k_2 are respectively shown in panels C and D as a function of [ImF], and in panels G and H as a function of [total Mg^{2+}].

MgF_4^{2-}, which cannot be found as such in aqueous solution. A similar interpretation was given by Antonny et al. [26], who stated that, although magnesium does not form (anionic) stable complexes with fluoride in aqueous solution, fluoride and magnesium can bind separately to form a gamma-phosphate analog in the G protein transducin.

4.3. A model for the formation of the E2·Pi-like state

We propose in Fig. 13 a scheme of the reactions involved in the formation of *E*2Mg–MgF_4. The model is not intended for giving a quantitative description of the phenomenon but rather to show the feasibility of the hypotheses used for its building.

All the reactions were considered as taking place in rapid equilibrium (species within the upper box and the shaded area in Fig. 13), with the exception of the conformational transitions between the *E*1 and *E*2 conformers, and the very last reactions that generate *E*2Mg–MgF_4, which include the binding of either MgF_2 or F^- to species in the *E*2 conformation. The scheme does not exclude the possibility of the existence of other species and pathways, but provided that these species are connected through rapid equilibrium reactions the simulated results will remain unchanged. In the model we have included MgF^+ as competing with Mg^{2+} for its binding to *E*1 and *E*2. The assumption of a random binding of these two ligands to form the species *E*1MgMgF and *E*2MgMgF was ruled out since it failed to improve the ability of the model for reproducing the experimental results. The present structure of the model could support the idea that MgF^+ binds to the site for Mg^{2+}, although this statement deserves a more thorough study.

Simulated curves based on this model are presented in Fig. 14 using the values of parameters shown in the figure legend. It can be seen that the qualitative behavior of the simulated time courses agrees very well with the results. The assumptions introduced in the model satisfy that: (*i*) the concentration of *E*1 relative to that of *E*2 is higher in the presence of Mg^{2+} than in its absence; (*ii*) the rate of the reaction *E*1Mg → *E*2Mg is lower than that of *E*1 → *E*2, which in turn is lower than that of *E*1MgF → *E*2MgF, *(iii)* the rate of formation of the *E*2Mg–MgF_4 complex is very low and increases along a hyperbolic or a parabolic function of [Mg^{2+}] and [F^-], respectively, and (*iv*) *E*2Mg–MgF_4 is a very stable complex.

In the model we propose that there is a very low affinity for the binding in rapid equilibrium of MgF_2 and F^- to the species in the *E*2 conformation of the ATPase, i.e. the values for the equilibrium dissociation constants K_{E2MgF2}, $K_{E2Mg2F2}$, and $K_{E2Mg2F3}$ are in the tens of millimolar to molar range (see legend to Fig. 14). Only the last elementary reactions leading to *E*2Mg–MgF_4 are of very high affinity for the ligands involved, i.e. the values of equilibrium dissociation constants (k_{iMg}/k_{Mg}) and (k_{iF}/k_F) are very small, 2.3×10^{-3} μM and 1×10^{-5} μM, respectively. These features of the model allow explaining both, the very low rate of formation and the high stability of the *E*2Mg–MgF_4 complex. In their work, Murphy and Hoover [3] suggested the occurrence of a slow structural rearrangement of the Na,K-ATPase after the equilibrium formation of the complex with fluoride. Later, Cornelius et al. [11] adopted the proposal of Murphy and Hoover by stating that, after the equilibrium binding of metal–fluoride complexes to the Na,K-ATPase, the resulting species undergoes a slow isomerization step leading to a very stable *E*2P-like state. Our results show that, although k_{obs} exhibit values that seem to be too low for a diffusion limited process under the conditions tested, these values continue to increase with the concentrations of magnesium and fluoride in a non-saturating manner. This and the good agreement between our simulated and experimental results call into question the need of a slow isomerization step in the formation of *E*2Mg–MgF_4.

4.4. Rb^+ occlusion

From the results in this work, two different actions of Mg^{2+} should be considered: one is the formation and coordination of a Pi-like compound in an intracellular domain of the Na,K-ATPase, bringing it to the *E*2Mg–MgF_4 complex, and the other is an apparent competition with Rb^+ for the cation sites. This second effect can explain the decrease in Rb_{occ} caused by Mg^{2+} in the presence of fluoride as well as in its absence [27]. Whether this effect is exerted from the extracellular access, as proposed by Laursen et al. [28], is still to be determined.

The reversion by fluoride of the drop in the equilibrium level of occluded Rb^+ caused by Mg^{2+} is reflecting the formation of *E*2(Rb_2)Mg–MgF_4 and resembles that obtained by addition of vanadate [23]. Unlike the *E*2P state that can be isolated under physiological conditions (the ground state), *E*2Mg–MgF_4 and *E*2Mg–vanadate are *E*2P-like states capable of occluding K^+.

In the Albers–Post model, it is assumed that the access to the transport sites is intracellular or extracellular for reaction intermediates in the *E*1 or the *E*2 conformation, respectively [1]. Since it has been shown that the rate constant of K^+ deocclusion in the presence of ATP is very close to the value measured for the *E*2 → *E*1 change, it is reasonable to think that K^+ is released through the intracellular access of the protein under these conditions (steps 4 through 6 in Fig. 1) [22,29]. On the other hand, in a medium with Na^+ but in the absence of the nucleotide, there is evidence showing that Rb^+ is being released before the *E*2 → *E*1 transition takes place, i.e. through the extracellular access [22,23]. Here we found that Rb^+ release from *E*2(Rb_2)Mg–MgF_4 upon Na^+ addition occurs at the same rate as that from *E*2(Rb_2) but is not accompanied by a conformational transition to *E*1. This difficulty to shift to *E*1 agrees with the inability of ADP to accelerate Rb^+ deocclusion from *E*2(Rb_2)Mg–MgF_4. In this regard, the combined effect of magnesium and fluoride is very similar to that of magnesium plus vanadate, producing states that allow a slow exchange of Rb^+ from the *E*2 conformation.

From the analysis of the time courses of Rb^+ occlusion, we propose that the *E*2Mg–MgF_4 complex mainly binds Rb^+ from the external access, which exists in an open (E_{open}) or in a closed form (E_{closed}), as shown in the following reaction sequence:

$$\begin{array}{c} E_{closed} \rightleftharpoons E_{open} \\ E_{open} + Rb^+ \rightleftharpoons E_{open}Rb \rightleftharpoons E_{closed}(Rb). \end{array}$$

The rate of occlusion will be a function of the rate constants of opening and closing of the empty and the Rb^+-bound forms, and the concentration of Rb^+. The low rate of occlusion observed in this work might be explained if the concentration of the empty open form, E_{open}, were a small fraction of the total enzyme concentration and/or if the rate limiting step in this sequence were the opening rate constant from E_{closed} to E_{open}. Occlusion of Rb^+ by *E*2Mg–MgF_4 is 5–8 times slower than that observed under similar conditions for the *E*2Mg–vanadate complex [23]. Considering the physiological dephosphorylation sequence, *E*2-P → *E*2 + Pi, this difference indicates that the product state (represented by *E*2Mg–MgF_4) is less prone to occlude Rb^+ than the transition state (mimicked by *E*2Mg–vanadate) and could provide a tool to discriminate between the intermediates in this sequence.

Transparency document

The Transparency document associated with this article can be found, in the online version.

Acknowledgments

The present work was supported by Agencia Nacional de Promoción Científica y Tecnológica (PICT 2012-1053), Consejo Nacional de Investigaciones Científicas y Técnicas (PIP 0706) and UBACYT-University of Buenos Aires (W 307). We thank Ms. Angielina Damgaard and Ms. Birthe B. Jensen, Department of Biophysics, University of Aarhus, Denmark, for preparing the Na,K-ATPase and Dr. Romina Carballo for helpful discussion on analytical chemistry topics.

Appendix A. Supplementary data

Supplementary data to this article can be found online at http://dx.doi.org/10.1016/j.bbamem.2015.03.023.

References

[1] I.M. Glynn, J.D. Karlish, Occluded cations in active transport, Annu. Rev. Biochem. 59 (1990) 171–205.
[2] S. Danko, K. Yamasaki, T. Daiho, H. Suzuki, Distinct natures of beryllium fluoride-bound, aluminum fluoride-bound, and magnesium fluoride-bound stable analogues of an ADP-insensitive phosphoenzyme intermediate of sarcoplasmic reticulum Ca^{2+}-ATPase: changes in catalytic and transport sites during phosphoenzyme hydrolysis, J. Biol. Chem. 279 (2004) 14991–14998.
[3] A.J. Murphy, J.C. Hoover, Inhibition of the Na,K-ATPase by fluoride. Parallels with its inhibition of the sarcoplasmic reticulum CaATPase, J. Biol. Chem. 267 (1992) (16995-16700).
[4] K. Abe, K. Tani, Y. Fujiyoshi, Structural and functional characterization of H^+, K^+-ATPase with bound fluorinated phosphate analogs, J. Struct. Biol. 170 (2010) 60–68.
[5] J. Bigay, P. Deterre, C. Pfister, M. Chabre, Fluoride complexes of aluminium or beryllium act on G-proteins as reversibly bound analogues of the gamma phosphate of GTP, EMBO J. 6 (1987) 2907–2913.
[6] J.D. Clausen, D.B. McIntosh, D.G. Woolley, J.P. Andersen, Modulatory ATP binding affinity in intermediate states of E2P dephosphorylation of sarcoplasmic reticulum Ca^{2+}-ATPase, J. Biol. Chem. 286 (2011) 11792–11802.
[7] C. Toyoshima, H. Nomura, T. Tsuda, Lumenal gating mechanism revealed in calcium pump crystal structures with phosphate analogues, Nature 432 (2004) 361–368.
[8] J.P. Morth, B.P. Pedersen, M.S. Toustrup-Jensen, T.L. Sørensen, J. Petersen, J.P. Andersen, B. Vilsen, P. Nissen, Crystal structure of the sodium–potassium pump, Nature 450 (2007) 1043–1049.
[9] T. Shinoda, H. Ogawa, F. Cornelius, C. Toyoshima, Crystal structure of the sodium-potassium pump at 2.4 A resolution, Nature 459 (2009) 446–450.
[10] J.D. Robinson, R.L. Davis, M. Steinberg, Fluoride and beryllium interact with the (Na^+/K^+)-dependent ATPase as analogs of phosphate, J. Bioenerg. Biomembr. 18 (1986) 521–531.
[11] F. Cornelius, Y.A. Mahmmoud, C. Toyoshima, Metal fluoride complexes of Na, K-ATPase: characterization of fluoride-stabilized phosphoenzyme analogues and their interaction with cardiotonic steroids, J. Biol. Chem. 286 (2011) 29882–29892.
[12] J.C. Skou, M. Esmann, Effect of magnesium ions on the high-affinity binding of eosin to the (Na^+/K^+)-ATPase, Biochim. Biophys. Acta 727 (1983) 101–107.
[13] J.C. Skou, M. Esmann, Eosin, a fluorescent probe of ATP binding to the (Na^+/K^+)-ATPase, Biochim. Biophys. Acta 647 (1981) 232–240.
[14] M.R. Montes, R.M. González-Lebrero, P.J. Garrahan, R.C. Rossi, Eosin fluorescence changes during Rb^+ occlusion in the Na^+/K^+-ATPase, Biochemistry 45 (2006) 13093–13100.
[15] I. Klodos, M. Esmann, R.L. Post, Large-scale preparation of sodium–potassium ATPase from kidney outer medulla, Kidney Int. 62 (2002) 2097–2100.
[16] R.E. Connick, M.-S. Tsao, Complexing of magnesium ion by fluoride ion, J. Am. Chem. Soc. 76 (1954) 5311–5314.
[17] N. Shibata, S.H. Sakaki, Y. Sigita, Theoretical study of magnesium fluoride in aqueous solution, J. Phys. Chem. B 115 (2011) 10553–10559.
[18] E. Rowatt, R.J. Williams, The interaction of cations with the dye arsenazo III, Biochem. J. 259 (1989) 295–298.
[19] R.C. Rossi, S.B. Kaufman, R.M. González-Lebrero, J.G. Nørby, P.J. Garrahan, An attachment for nondestructive, fast quenching of samples in rapid-mixing experiments, Anal. Biochem. 270 (1999) 276–285.
[20] K.P. Burnham, D.R. Anderson, Model selection and Multimodel Inference: A Practical Information-theoretic Approach, Springer, New York, 2002. 66–67.
[21] S. Hoops, S. Sahle, R. Gauges, C. Lee, J. Pahle, COPASI—a complex pathway simulator, Bioinformatics 22 (2006) 3067–3074.
[22] B. Forbush III, Rapid release of 42 K or 86Rb from two distinct transport sites in the Na, K-pump in the presence of Pi or vanadate, J. Biol. Chem. 262 (1987) 11116–11127.
[23] M.R. Montes, J.L. Monti, R.C. Rossi, E2 → E1 transition and Rb^+ release induced by Na^+ in the Na^+/K^+-ATPase. Vanadate as a tool to investigate the interaction between Rb^+ and E2, Biochim. Biophys. Acta 1818 (2012) 2087–2093.
[24] G. Goldstein, Equilibrium distribution of metal–fluoride complexes, Anal. Chem. 36 (1964) 243–244.
[25] D.L. Graham, P.N. Lowe, G.W. Grime, M. Marsh, K. Rittinger, S.J. Smerdon, S.J. Gamblin, J.F. Eccleston, MgF_3^- as a transition state analog of phosphoryl transfer, Chem. Biol. 9 (2002) 375–381.
[26] B. Antonny, J. Bigay, M. Chabre, A novel magnesium-dependent mechanism for the activation of transducin with fluoride, FEBS 268 (1990) 277–280.
[27] R.M. González-Lebrero, S.B. Kaufman, P.J. Garrahan, R.C. Rossi, The occlusion of Rb+ in the Na, K-ATPase II. The effects of Rb+, Na+, Mg2+, or ATP on the equilibrium between free and occluded Rb+, J. Biol. Chem. 277 (2002) 5922–5928.
[28] M. Laursen, L. Yatime, P. Nissen, N.U. Fedosova, Crystal structure of the high-affinity Na^+K^+–ATPase–ouabain complex with Mg^{2+} bound in the cation binding site, Proc. Natl. Acad. Sci. U. S. A. 110 (2013) 10958–10963.
[29] B. Forbush III, Rapid release of 42 K and 86Rb from an occluded state of the Na, K-pump in the presence of ATP or ADP, J. Biol. Chem. 262 (1987) 11104–11115.